



Article

---

# Study of the Evolution of the Performance Ratio of Photovoltaic Plants Operating in a Utility-Scale Installation Located at a Subtropical Climate Zone Using Mixed-Effects Linear Modeling

---

Carlos Montes, Roberto Dorta-Guerra, Benjamín González-Díaz, Sara González-Pérez, Luis Ocaña and Elena Llarena

## Topic

Advances in Renewable Energy Technologies and Systems Solutions






Edited by

Dr. Doug Arent, Dr. Adam Warren and Prof. Dr. Xiaolei Yang



## Article

# Study of the Evolution of the Performance Ratio of Photovoltaic Plants Operating in a Utility-Scale Installation Located at a Subtropical Climate Zone Using Mixed-Effects Linear Modeling

Carlos Montes <sup>1,2,\*</sup> , Roberto Dorta-Guerra <sup>3</sup> , Benjamín González-Díaz <sup>2</sup> , Sara González-Pérez <sup>4</sup> , Luis Ocaña <sup>1,2</sup>  and Elena Llarena <sup>1</sup>

<sup>1</sup> Instituto Tecnológico y de Energías Renovables, S. A. (ITER), 38600 Granadilla, Spain

<sup>2</sup> Departamento de Ingeniería Industrial, Escuela Superior de Ingeniería y Tecnología, Universidad de La Laguna (ULL), 38200 La Laguna, Spain

<sup>3</sup> Departamento de Matemáticas, Estadística e Investigación Operativa, Facultad de Ciencias, Universidad de La Laguna (ULL), 38200 La Laguna, Spain

<sup>4</sup> Departamento de Didácticas Específicas, Universidad de La Laguna (ULL), 38200 La Laguna, Spain

\* Correspondence: cmontes@iter.es; Tel.: +34-922-747-700

**Abstract:** This paper assessed the evolution of the performance ratio (PR) of a utility-scale photovoltaic (PV) installation that operates at subtropical climate conditions. The period of study encompassed 8 years, and the PR was calculated according to the ICE 61724 standard with a monthly resolution. A linear mixed effects model (LME) is a suitable tool for analyzing longitudinal data. Three LME models were assessed to provide the degradation rate. The “null model” evaluates the general relationship between PR and time with a monthly declination rate ( $\Delta PR\%$ ) of 0.0391%/month. The “typology model” considered the relationship between PR and, as covariates, time, *Manufacturer*, *Technology*, and *NominalP*. Only the  $\Delta PR\%$  related to *NominalP* was found to be significant, so that, when the nominal power of a type of PV module used for a PV production unit is increased by one unit, the  $\Delta PR\%$  of the corresponding unit increases by 0.000897%/month. Finally, the “location model” took into account the relationship between PR and, as covariates, time, *Edge*, and *LengthSt*. These last two factors were significant, resulting in an increase of 0.0132%/month for a PV unit located at the edge of the facility and 0.00117%/month and per PV production unit when considering the length of a street, respectively.

**Keywords:** solar photovoltaic; performance ratio; PV module degradation; mixed-effect linear modeling



**Citation:** Montes, C.; Dorta-Guerra, R.; González-Díaz, B.; González-Pérez, S.; Ocaña, L.; Llarena, E. Study of the Evolution of the Performance Ratio of Photovoltaic Plants Operating in a Utility-Scale Installation Located at a Subtropical Climate Zone Using Mixed-Effects Linear Modeling. *Appl. Sci.* **2022**, *12*, 11306. <https://doi.org/10.3390/app122111306>

Academic Editors: Doug Arent, Xiaolei Yang and Adam Warren

Received: 13 October 2022

Accepted: 4 November 2022

Published: 7 November 2022

**Publisher's Note:** MDPI stays neutral with regard to jurisdictional claims in published maps and institutional affiliations.



**Copyright:** © 2022 by the authors. Licensee MDPI, Basel, Switzerland. This article is an open access article distributed under the terms and conditions of the Creative Commons Attribution (CC BY) license (<https://creativecommons.org/licenses/by/4.0/>).

## 1. Introduction

The study of the reliability and long-term durability of photovoltaic (PV) modules has a great impact on the energy forecast, the economics of the power plants, and the planning of the operation and maintenance activities of the PV systems [1–3].

Different performance analyses have been carried out with different technologies, plant topology, and placements [4–9], wherein the results indicate the PV modules have provided electric power for more than 20 years. However, errors determining degradation rates can increase financial risks in the PV sector [10].

In outdoor conditions, to determine how long a PV module or system will last is a challenge because they are influenced by several issues, such as the local climate, technology, materials, and manufacturing, as much as the installation conditions themselves [11].

After more than 40 years of field testing, in different world locations, degradation rate distribution of the PV power plants have reported around 0.5%/year [10,12,13]. Therefore, this value has been also adopted to consider long-term crystalline silicon PV module degradation in financial models [14]. Lately, annual degradation rates have been estimated on PV modules, using modern cell technologies as well as encapsulating techniques,

which reduced the average degradation rate at 0.4%/year [15], wherein values lower than 0.27%/year can be achieved for crystalline silicon technologies, operating in utility-scale PV facilities subjected to proper operation and maintenance practices [16].

To perform an analysis of the durability, several parameters are required to evaluate the degradation, such as the I-V curve evolution [15], color change of the PV panels [17], or the temperature coefficient variation [18], among other approaches. However, the analysis of the performance ratio (PR) is one of the most widely used methods [11,19–24], mainly due to its accuracy and non-dependence of external factors.

Since a single set of degradation measurements based on one measurement are not representative of the population to estimate true degradation of a PV installation, repeated measures across several groups are necessary. The analysis of the operation data and performance through linear mixed effects models (LEMs) is a suitable tool for analyzing longitudinal data to explain the degradations in PV modules/systems [25]. Even more, it is reasonable to assume a linear degradation model, although some publications use an exponential degradation model [26] or classical series decomposition [20]; it is shown that for a typical starting degradation rate, these models do not differ significantly during the first 10–15 years [27].

In this paper, the performance of 8 years of a 13 MW installation located in the South of Tenerife (Canary Islands, Spain) was analyzed. LEM approaches were used to evaluate the evolution of the PR of the PV production units in which this facility is articulated, and its degradation rate, considering the effects of technology, manufacturer, and nominal power of photovoltaic modules used during its installation, as well as the distribution of said PV units within the facility. The concept of degradation rate is used in this work, wherein robust estimation of the true degradation in a specific environment was evaluated [28].

## 2. Materials and Methods

### 2.1. Description of the Photovoltaic System

The analysis of the PR and its degradation rate was performed in SOLTEN, a 20 MW utility-scale PV facility located in the south of Tenerife, Canary Islands, in the municipality of Granadilla (see Figure 1), which was installed and operated by the Instituto Tecnológico y de Energías Renovables, S.A. (ITER). The Canary Islands are located in the trade wind zone on the southeastern side of the Azorean anticyclonic system, but also relatively near to the West Coast of Africa. As a result, the islands have a subtropical climate, characterized by hot summers and mild winters with infrequent frost. However, due to the island's orography, they are also subjected to other climates that have a local effect, called microclimates [29]. Thus, according to the Köppen climate classification [30], the climate where the PV facility is located is similar to hot arid desert, with high levels of solar irradiation, but, due to its closeness to the coast, it is also heavily exposed to a salty and humid environment.

The SOLTEN 20 MW PV facility was developed on a plot of land of 217,775.80 m<sup>2</sup> between 2006 and 2008 and is made up of 200 PV generation units. Each unit has 100 kW of nominal power, occupies an area of about 820 m<sup>2</sup>, and is set up at 10° tilt and true North–South orientation. In all units, the PV modules are clamped to light aluminum structures, totally modular and removable, being formed of pillars, girders, and beams, mounted over profiles of galvanized steel, embedded on concrete foundations (see Figure 2).

The PV production units were placed in rows, leaving streets between each row of plants, both to minimize the impact of shadows and to allow their servicing. Since the plot of land has a diamond-like shape, each row accommodated a different number of plants, depending on its location. Following the nomenclature adopted by the SOLTEN maintenance teams, henceforth the term “street” will be used to refer to both a row of PV units and the transiting path that lies at the south of each row.

The inverters used in all the PV production units are Teide 100 [31], developed and manufactured by ITER. Teide 100 is a 100 kW rated, transformer-less inverter, especially designed for facilitating its operation and maintenance, as well as to contribute to maintain

the grid through the voltage drop during exceptional conditions, such as voltage dips, according to the Spanish Grid Codes.

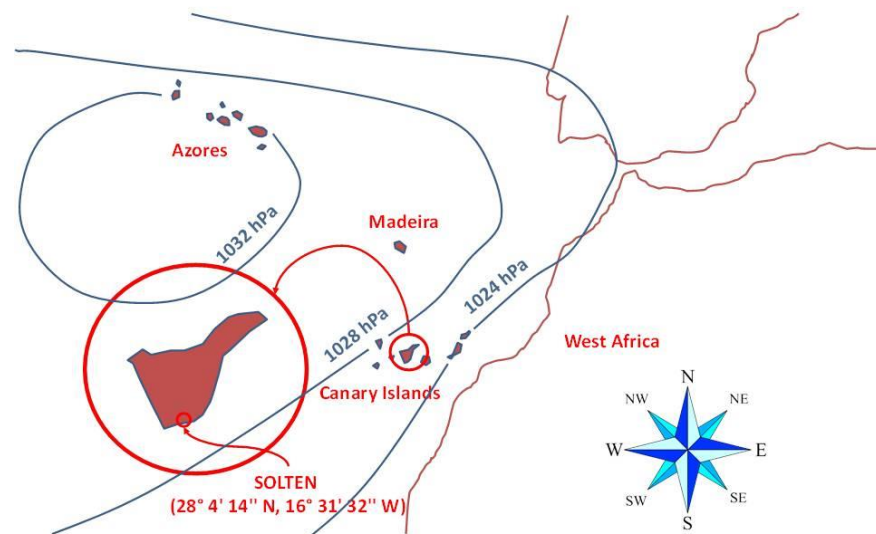


**Figure 1.** Geographical location of the SOLTEN PV installation (own elaboration).



**Figure 2.** Image depicting a typical distribution of PV production units in the SOLTEN PV installation (own elaboration).

The PV production units are connected to a SCADA (Supervisory Control and Data Acquisition) system, which monitors the inverters; the security equipment; the energy meters; and, since 2011, also a weather station located at the facilities that has, among other sensors, a ISO 9060 spectrally flat Class B pyranometer (CMP6 by Kipp and Zonen), which was placed, oriented, and tilted as the PV plants. All the acquired data are securely stored in a database.

As can be seen in Figure 3, SOLTEN 20 MW is divided in two phases: SOLTEN I (13 MW) and SOLTEN II (7 MW), which differ only in the way in which the energy injected into the grid is accounted for. Thus, while SOLTEN I is articulated around 130 PV units, each one serviced by a class B in active energy meter (according to European Directive MID EN 50470 or class 1 according to IEC-62053-2) that is connected to the low-voltage grid, SOLTEN II has 70 PV units that are all serviced by one single energy meter instead, which is connected to the medium voltage grid. Because of this difference, the present study had to be restricted only to the SOLTEN I phase.

The reason behind this configuration around 100 kW production units has to do with the kind of business model applied during the promotion and construction of the facilities, which was conceived in order to make use of the most suitable feed-in tariffs available at the time [32]. Thus, the installation was articulated as a collective solar farm,

wherein the PV generation units (the PV modules; the structures; the inverters; and, for phase I, also the electric meters) were individually purchased by different owners, while the remaining infrastructure (the transform stations, the high-voltage evacuation lines, the communications, the security, and the fire control systems, among other services) were shared by all the owners [33].

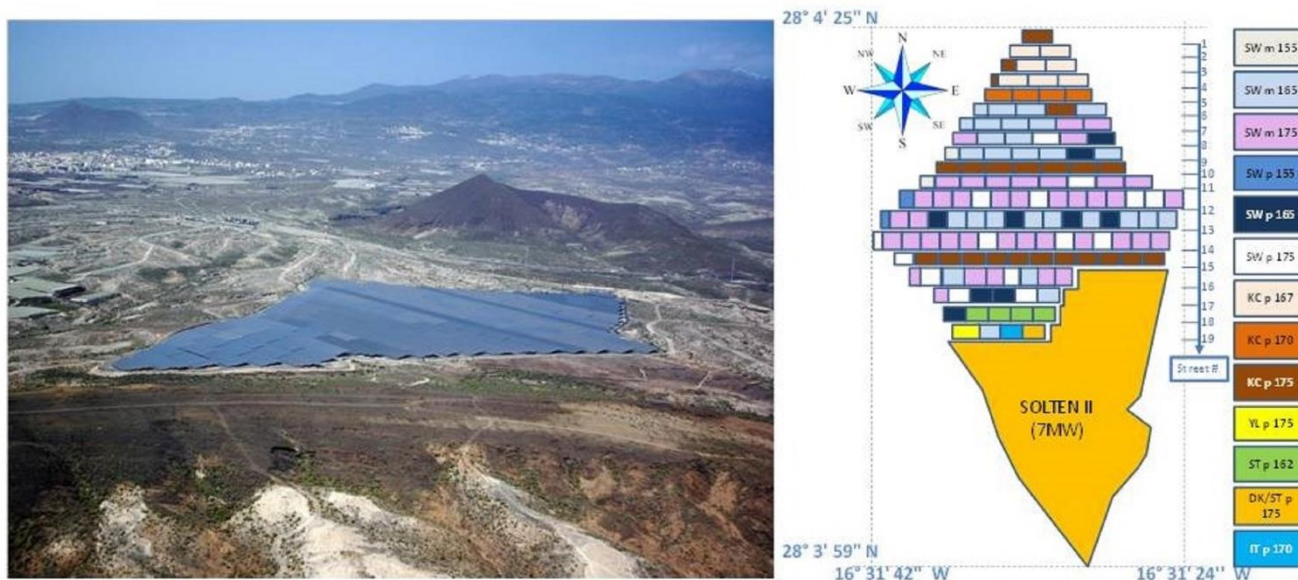


**Figure 3.** Aerial view of the SOLTEN 20 MW PV installation (left) and a diagram highlighting SOLTEN I (13 MW), as well as its distribution in streets and PV units, as a function of the type of module installed (right). Own elaboration.

## 2.2. PV Facilities under Study

As explained above, this study focused on the SOLTEN I phase (13 MW) that, in total, has 130 PV production units of 100 kW each. In this phase, 81,560 PV modules, made with mono or polycrystalline cells and provided by four different manufacturers, ranging from 175 W to 155 W of nominal power, were installed. All the installed modules with monocrystalline technology were formed by 72  $125 \times 125$  mm cells connected in series, while the majority of the installed modules that carry polycrystalline cells had 48  $156 \times 156$  mm cells, also associated in series. In both cases, the module fabrication process applied modern lamination techniques, with encapsulations consisting of solar glass, interlayer sheets of ethyl vinyl acetate (EVA), and three-layer backing film, made of two polyvinyl fluoride films (PVF) that sandwich a polyethylene terephthalate (PET) layer, usually called TPT (tedlar®-polyester-tedlar®). It is important to notice that these photovoltaic modules were not mixed, that is, each of the 130 PV production units was installed using a single variety of those that were available. Thus, one way to identify one PV production unit from another could be by considering the manufacturer of the modules used for its installation, the type of cells that were used for the modules' lamination (which we have referred to as "technology" here), and their corresponding nominal power (see Table 1).

Moreover, the PV production units were installed in straight rows, placed from east to west, called streets. The number of units per street varied in order to adapt to the available plot of land. Thus, another way to identify one PV production unit from another could be by considering its belonging to a determined street, as much as its particular location within that street. Regarding this topic, it is important to notice that from street 16 to 19, the eastern side of each street had PV production units that belong to SOLTEN II and, therefore, the units belonging to SOLTEN I start somewhere in the middle of these streets (see Table 2).

**Table 1.** Distribution of the modules installed in SOLTEN I, considering manufacturer (SW, KC, YL, ST, DK/ST, and IT); technology (“m” for monocrystalline and “p” for polycrystalline); nominal power, number of PV production units installed with these modules; and the total number of modules installed for each type.

Manufacturer	Technology	Nominal Power (W)	N° of PV Units	N° of Modules	Cell Size (mm)
SW	m	155	1	684	125 × 125
		165	24	15,526	
		175	40	24,529	
		155	1	684	
		165	9	5814	
		175	15	9158	
KC	p	167	7	4522	156 × 156
		170	4	2584	
		175	21	12,938	
YL		175	1	648	
ST		162	5	3190	
DK/ST		175	1	616	
IT		170	1	667	

**Table 2.** Number of PV production units per street in SOLTEN I. Note that from street number 16 to 19, there are units that belong to SOLTEN I and SOLTEN II. The former are located on the west side, and the latter on the east side of each street.

Street #	SOLTEN I	SOLTEN II	Total # of PV Units
1	1	0	1
2	2	0	2
3	3	0	3
4	3	0	3
5	4	0	4
6	5	0	5
7	5	0	5
8	6	0	6
9	7	0	7
10	7	0	7
11	8	0	8
12	15	0	15
13	15	0	15
14	15	0	15
15	12	0	12
16	8	5	13
17	5	4	9
18	5	4	9
19	4	4	8

### 2.3. Performance Ratio Calculation

The IEC 61724 norm constitutes the European Standard that describes the general recommendations for performance monitoring and analysis of PV systems [19], both for grid tied and for isolated forms. Thus, in order to provide information on the energy efficiency and reliability of a PV installation, the standard defines a performance ratio (*PR*) as the quotient of the system’s final yield ( $Y_f$ ) to its reference yield ( $Y_r$ ), and indicates the

overall effect of losses on the system output due to both array temperature and system component inefficiencies or failures, including balance of system components.

The PR is defined as

$$PR = \frac{Y_f}{Y_r} = \left( \frac{E_{out}}{P_0} \right) / \left( \frac{H_i}{G_{i,ref}} \right) \tag{1}$$

where the  $E_{out}$  is the net energy output of the entire PV system (AC in kWh); the  $P_0$  is the rated kW (DC in kWp) of the installed PV array; the  $H_i$  is the total in-plane irradiation (in kWh·m<sup>-2</sup>) during the considered period; and, finally,  $G_{i,ref}$  is the module’s reference plane of array irradiance (1 kW·m<sup>-2</sup>), which is the irradiance at which  $P_0$  is determined.

Thus, since the available data had monthly resolution, the monthly performance ratio,  $PR_{monthly}$ , or simply PR henceforth, is the performance ratio, evaluated for a reporting period of one month.

### 2.4. Data Filtering

From the available data, which encompasses from January 2012 to December 2019, 8 operation years, the monthly performance ratio (PR) was calculated for the 130 PV production units, following the formulation indicated in the previous section.

The dataset available from the beginning of 2020 to the present was not considered in this study due to the arrival of the COVID-19 pandemic on the island, which resulted in a reduction in energy consumption. Since the electrical system of Tenerife is islanded, the energy production must be finely tuned to the expected consumption. This important task is carried out by Red Eléctrica de España [34]. As a consequence of the reduction in consumption, this institution began to order curtailments to all the island’s energy producers, which also affected SOLTEN.

From the 130 PV production units initially sampled, described in Tables 1 and 2, and to study the effect of the manufacturer on the performance ratio evolution, the units of type ST (5 plants), DK/ST (1 plant), IT (1 plant), and YL (1 plant) were discarded for not having sufficient representativeness.

Therefore, the number of plants considered in this study was reduced to 122 and aggregated depending on their module manufacturer, nominal power, and technology, as shown in Tables 3–5, respectively. Representativeness of each considered variable is shown in each table.

**Table 3.** Distribution of the PV production units, considering the manufacturer’s representativeness.

Manufacturer	Technology	Nominal Power (W)	N° of PV Units	Representativeness
SW	m	155	1	73.77%
		165	24	
		175	40	
	p	155	1	
		165	9	
		175	15	
KC	p	167	7	26.23%
		170	4	
		175	21	

Outlier and extreme points were analyzed by inspecting the box-and-whisker plots (see Figure 4). PR values greater than 1 were discarded from the study. The absence of a comprehensive historical record about the operation and maintenance actions carried out in the facilities made it impossible to ascertain causes to explain the existence of these anomalous PR values. In some instances, PR values of 1 and above could be attributed to

momentary malfunctions on either the electric meters or in the data acquisition and storage procedures, shifting part of the monthly energy production on a PV production unit onto the following month.

**Table 4.** Distribution of the PV production units, considering their nominal power’s representativeness.

Nominal Power (W)	Manufacturer	Technology	N° of PV Units	Representativeness
155	SW	m	1	1.64%
		p	1	
165	SW	m	24	27.05%
		p	9	
167	KC	p	7	5.74%
170	KC	p	4	3.28%
175	SW	m	40	62.30%
		p	15	
	KC	p	21	

**Table 5.** Distribution of the PV production units, considering the technology’s representativeness.

Nominal Power (W)	Manufacturer	Technology	N° of PV units	Representativeness
m	155		1	53.28%
	165	SW	24	
	175		40	
P	155	SW	1	46.72%
	165	SW	9	
	167		7	
	170	KC	4	
			21	
	175	SW	15	

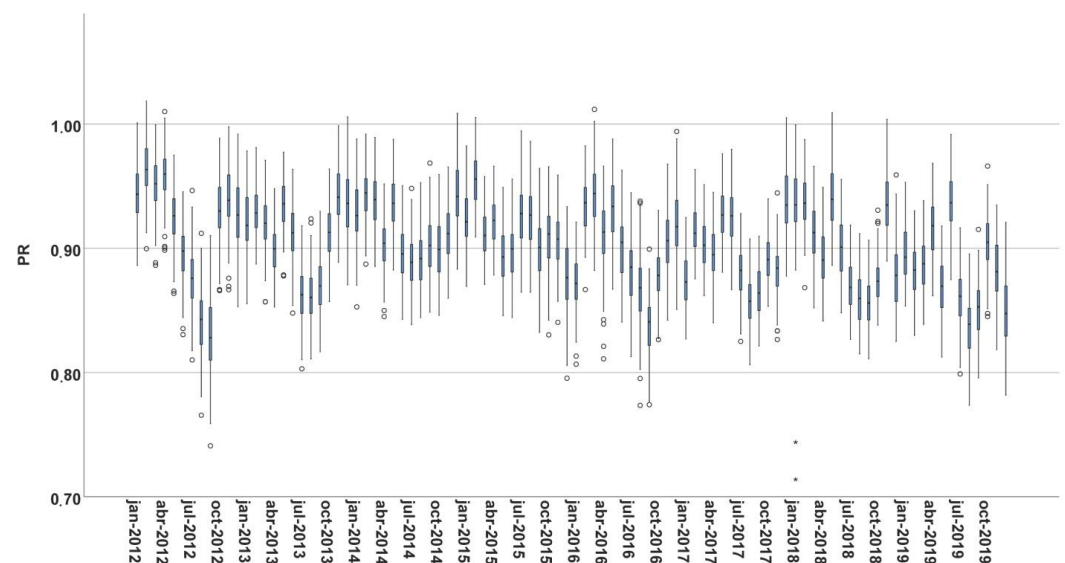


**Figure 4.** Monthly PR of 130 production units over the period January 2012–December 2019 installed in SOLTEN I. The values that represent potential outliers and extreme outliers are marked with points (o) and asterisks (\*), respectively. Own elaboration.



### 2.5. Performance Loss Rate Evaluation Using Mixed-Effects Linear Models

A random coefficients model (mixed-effects linear model) with random intercept and slope was applied to monthly PR. Three models were defined to evaluate the PR decline rate over time, or  $\Delta PR\%$ . The first model, denoted as “null model”, was constructed to evaluate the  $\Delta PR\%$  when no factors were included. The second model, denoted as “typology model”, was devised to evaluate the  $\Delta PR\%$  when factors related to the nature of the modules used in the PV production units were taken into account. To that effect, three covariates were considered: module manufacturer (*Manufacturer*), type of cell used in the modules’ lamination (*Technology*), and the nominal power of the modules (*NominalP*) installed at each PV production unit. The third model, denoted as “location model”, was conceived to evaluate the  $\Delta PR\%$  when factors related to the situation of the PV production units, within the facility, were taken into account. Thus, it included two covariates: the edge effect (*Edge*), which takes into account whether or not a PV production unit is located at the facility’s eastern border and, therefore, contemplates the impact of being more exposed to local conditions, such as the prevailing winds that this area has (see Figure 5), and the length of the street effect (*LengthSt*), which evaluates the consequences of having a different number of PV production units per street within the installation.

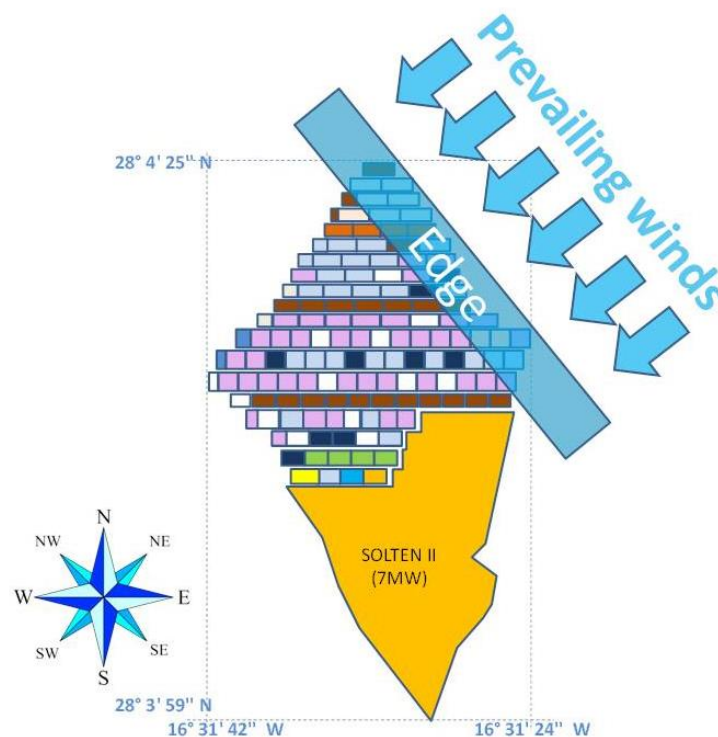


**Figure 5.** Diagram depicting the SOLTEN facility together with the zone considered as the “edge area” in terms of direct exposure to the prevailing winds. Own elaboration.

Evaluation of the principal effects and interactions of these variables over time allowed to calculate the PR decline rate ( $\Delta PR\%$ ). For this model, the homoscedasticity was assessed by visual inspection of a scatterplot of residuals versus fitted values. The assumption of normality was met, as assessed by the histogram of residuals and by the Kolmogorov test ( $p > 0.05$ ).

#### Performance Ratio Declination Rate Model

Let  $y_{ij}$  be the measured performance ratio (*PR*) of plant  $i$  at time  $t_{ij}$  in months, where  $i = 1, \dots, 122$  denotes number of PV production units and  $j$  denotes the considered period

with  $j = 1, \dots, m_i$ , where  $m_i \leq 96$ , that is, from January 2012 until December 2019. The linear degradation model is given by

$$y_{ij} = b_{0,i} + b_{1,i} t_{ij} + \varepsilon_{ij} \tag{2}$$

where  $b_{0,i}$  and  $b_{1,i}$  denote the intercept and the gradient of the linear model for plant  $i$ , respectively, and  $\varepsilon_{ij}$  denotes a random effect, and moreover,

$$\begin{aligned} b_{0,i} &= \beta_0 + b_{0,i}^* \\ b_{1,i} &= \beta_1 + b_{1,i}^* \end{aligned}$$

where

$$\begin{aligned} \beta_0 &= \gamma_{00} + \gamma_{01}x_{i1} + \dots + \gamma_{0k}x_{ik} \\ \beta_1 &= \gamma_{10} + \gamma_{11}x_{i1} + \dots + \gamma_{1k}x_{ik} \end{aligned}$$

and  $x_{ik}$  are the covariates for the “typology” model:  $x_{i1} = \text{“Manufacturer”}$ ;  $x_{i2} = \text{“Technology”}$ ;  $x_{i3} = \text{“NominalP”}$  and “location” model:  $x_{i1} = \text{“Edge”}$ ;  $x_{i2} = \text{“LengthSt”}$ .

The “null” model only assesses the relation between the PR and time.

The intercept and the gradient can be modeled using a bivariate normal distribution,  $(b_0, b_1)^t \sim \text{BVN}(\boldsymbol{\beta}, \mathbf{V})$  with mean vector

$$\boldsymbol{\beta} = (\beta_0, \beta_1)^t$$

and covariance matrix

$$\mathbf{V} = \begin{pmatrix} \sigma_{b_0}^2 & \text{Cov}(b_0, b_1) \\ \text{Cov}(b_1, b_0) & \sigma_{b_1}^2 \end{pmatrix}$$

Equation (2) can be written as a linear mixed model:

$$y_{ij} = \gamma_{10} + \gamma_{11}x_{i1} + \dots + \gamma_{1k}x_{ik} + \gamma_{10}t_{ij} + \gamma_{11}x_{i1}t_{ij} + \dots + \gamma_{1k}x_{ik}t_{ij} + (b_{0,i}^* + b_{1,i}^*t_{ij} + \varepsilon_{ij}) \tag{3}$$

The above Equation (3) can be written into matrix form:

$$\mathbf{Y}_i = \mathbf{X}_i\boldsymbol{\beta} + \mathbf{Z}_i\mathbf{b}_i^* + \boldsymbol{\varepsilon}_i \tag{4}$$

where

$$\begin{aligned} \mathbf{Y}_i &= (y_{i1}, \dots, y_{im_i})^t; \boldsymbol{\varepsilon}_i = (\varepsilon_{i1}, \dots, \varepsilon_{im_i})^t; \mathbf{b}_i^* = (b_{0,i}^*, b_{1,i}^*)^t; \\ &\quad (b_{0,i}^*, b_{1,i}^*)^t \sim \text{BVN}(\mathbf{0}, \mathbf{V}) \\ &\quad \boldsymbol{\varepsilon}_i \sim \text{MVN}(\mathbf{0}, \sigma^2\mathbf{I}_i); \\ &\quad \mathbf{v}(\mathbf{b}_i^*, \boldsymbol{\varepsilon}_i) = \mathbf{0}; \\ \mathbf{X}_i = \mathbf{Z}_i &= \begin{pmatrix} 1 & t_{i1} \\ \vdots & \vdots \\ 1 & t_{im_i} \end{pmatrix} \end{aligned}$$

and  $\mathbf{I}_i$  is a  $m_i$  by  $m_i$  identity matrix. Under this,  $\mathbf{Y}_i$  has a multivariate normal distribution with mean vector  $\mathbf{X}_i\boldsymbol{\beta}$  and covariance

$$\boldsymbol{\Sigma}_i = \mathbf{v}(\mathbf{Y}_i) = \mathbf{Z}_i\mathbf{V}\mathbf{Z}_i^t + \sigma^2\mathbf{I}_i \tag{5}$$

### 3. Results and Discussion

As can be seen in Table 6, the value obtained for the mean slope of the PR (or  $\Delta PR\%$ ) of the PV production units or the considered period at a monthly resolution, without considering any factor or covariable (null model), was 0.0391%/month. This is a remarkable result because, to our knowledge, it has not been reported with such accuracy and with this level of resolution thus far. Considering yearly intervals instead, the resulting value of the  $\Delta PR\%$  was 0.4692%/year. This is also relevant because it means that, despite the

challenging conditions in which the studied PV production units operate, in terms of exposure to high levels of irradiation and under quite harsh climatic environments, the obtained  $\Delta PR\%$  per year is slightly lower than 0.5%/year, which is the median value reported by Jordan and Kurtz after analyzing 2000 degradation rates, available in the literature, which were measured on individual modules or entire systems [13].

**Table 6.**  $\Delta PR$  estimation for the three mixed models: null model without covariates; typology model with covariates *Manufacturer*, *Technology*, and *NominalP*; and the location model with covariates *Edge* and *LenghtSt*. SE: standard error; 95% CI: 95% confidence interval.

Model	Covariates	Estimation $\Delta PR$ (month)	SE	p-Value	95% CI	
Null	Time	$-3.910 \times 10^{-4}$	$1.673 \times 10^{-5}$	<0.001	$-4.230 \times 10^{-4}$	$-3.580 \times 10^{-4}$
Typology	Time	$-2.370 \times 10^{-4}$	$6.257 \times 10^{-5}$	<0.001	$-3.600 \times 10^{-4}$	$-1.150 \times 10^{-4}$
	Manufacturer	$-5.118 \times 10^{-5}$	$4.811 \times 10^{-5}$	0.287	$-1.450 \times 10^{-4}$	$4.312 \times 10^{-5}$
	Technology	$1.271 \times 10^{-5}$	$4.204 \times 10^{-5}$	0.762	$-6.968 \times 10^{-5}$	$9.511 \times 10^{-5}$
	NominalP	$-8.977 \times 10^{-6}$	$3.289 \times 10^{-6}$	0.006	$-1.542 \times 10^{-5}$	$-2.529 \times 10^{-6}$
Location	Time	$-3.960 \times 10^{-4}$	$5.130 \times 10^{-5}$	<0.001	$-4.970 \times 10^{-5}$	$-2.960 \times 10^{-4}$
	Edge	$1.320 \times 10^{-4}$	$5.062 \times 10^{-5}$	0.009	$3.292 \times 10^{-5}$	$2.310 \times 10^{-4}$
	LenghtSt	$-1.177 \times 10^{-5}$	$3.755 \times 10^{-6}$	0.002	$-1.913 \times 10^{-5}$	$-4.412 \times 10^{-6}$

When considering the PR of the PV production units, this time by taking into account the module manufacturer (*Manufacturer*, in this case two manufacturers: “SW” and “KC”), the technology (*Technology*, that is, whether the modules were laminated with monocrystalline “m” or polycrystalline “p” cells), and the nominal power (*NominalP*, ranging from 155 to 175 W) as covariates, that is, the typology model, the results indicate that although the effect of the manufacturer and technology were not significant, when the nominal power of a type of PV module used is increased by one unit, the variation of the PR of the corresponding PV production unit per elapsed month decreases by 0.000897% (see Table 6).

Although this may look like a rather small number, according to this result and by considering it on an annual basis, its effect adds up so that, throughout the considered period, a PV production unit that has 175 W modules was, on average, 0.2153%/year below one who was made with 155 W ones (see Figure 6). In economic terms and by considering the tariff granted by the regulation in force at the time of completion of the installation [35], this means that by the year 2019, a PV production unit that has 175 W modules earned, on average, EUR 11.02/kW less than one that has 155 W.



**Figure 6.** Variation of the PR for PV production units made with modules of 155 W to 175 W per elapsed month. Own elaboration.

Now, taking into account how large the SOLTEN I facility is, where it was placed, and the way that the PV production units were distributed in it, the location model was

implemented with the covariates: *Edge* (to distinguish between PV production units that were placed at the easternmost border of the facility from those who were not in this position) and *LengthSt* (to evaluate the impact of having different number of PV production units per street). Thus, considering the *Edge* covariate, it was found that the monthly  $\Delta PR\%$  of a PV production unit located at the easternmost edge (or border) was 0.0132% higher than those not located at such position (or no border) (see Table 6).

Moreover, by considering this result on a yearly period, this difference becomes 0.1584% (see Figure 7). Again, in economic terms, this means that, by the year 2019, a PV production unit located at the easternmost border earned, on average, EUR 8.11/kW less than one not located at such a position.



**Figure 7.** Variation of the PR for a PV production unit located or not placed at the edge per elapsed month. Own elaboration.

Finally, taking into account the *LengthSt* covariate, the results indicate that the number of PV production units per street also influences their  $\Delta PR\%$ . In fact,  $\Delta PR\%$  increases, on average, by 0.00117% per month for each PV unit that increases the length of the street (see Table 6 and Figure 8).



**Figure 8.** Variation of the PR for PV production units in streets that have 1 to 15 units per elapsed month. Own elaboration.

As before, this is an effect that also adds up; thus, for instance, a street that has 10 PV production units was, on average 0.1264%/year above one who has just one PV unit. In economic terms, this means that, by 2019, having a street with 10 PV production units is supposed to earn, on average, EUR 6.41/kW less than having one made with only a single PV unit.

The last two results reflect the effect of exposure to the prevailing winds, which are the trade winds that blow from the northeast most of the year in this area. On the one hand, those winds help to transport particles of dust and ambient humidity, which become fixed mainly to those PV production units who are more exposed (which are the ones located by

the easternmost border of the installation), contributing to their soiling. On the other hand, those winds also provide a cooling mechanism to the PV production units that is more efficient the fewer units there are per street. Thus, a good practice for the operation and maintenance of these PV production units would be to take special care in cleaning those that have their east side free of obstacles. In addition, a more convenient way to install new photovoltaic units in this geographical area would be to locate them in the shortest possible streets or, if this is not feasible, to group them within the same street, so that there are free spaces between them.

#### 4. Conclusions

In this work, a study of the monthly declination rate of the PR (or  $\Delta PR\%$ ) of a utility-scale photovoltaic installation that operates in a subtropical climate (located on the south-east coast of Tenerife, Canary Islands) during a period of 8 years is presented.

Three models were defined. The “null model” directly considers the relationship between PR and time, which resulted in a  $\Delta PR\%$  of 0.0391%/month. This is a very relevant result because, to our knowledge, a monthly decline rate of the PR for PV installations has not been reported in the literature. Moreover, on an annual basis, this figure translates to 0.4692%/year, which is slightly below the degradation rates reported when analyzing individual modules or entire PV systems operating elsewhere, despite having the installation working in considerably harsh conditions, both in terms of irradiation and climatic exposure. This is an interesting result for energy stakeholders interested in sustainable energy investments, since it indicates the suitability of establishing these types of facilities in this kind of environment.

Considering that during the construction of the facilities, modules of different types were used, the “typology model” studied the relationship between PR and, as covariates, three factors (*Manufacturer*, *Technology*, and *NominalP*) and time. The results indicated that only the  $\Delta PR\%$  related to *NominalP* was significant, so that when the nominal power of a type of PV module used is increased by one unit, the variation of the PR of the corresponding PV production unit per elapsed month decreases by 0.000897%. Thus, for instance, a PV production unit that was built with 175 W modules presents, on average, a  $\Delta PR\%$  0.2153%/year lower than one that was built with modules of 155 W.

Taking into account the geographical situation of the facility, its size, and the distribution of the PV production units within it, the “location model” considers the relation between PR and, as covariates, two factors (*Edge* and *LengthSt*) and time. The results indicated that both covariates were significant. Thus, for the *Edge* one, the variation of the PR of a PV production unit located at the easternmost edge (or border) per elapsed month was, on average, 0.0132% larger than for one not located at such position. Again, on an annual basis, this value translates to 0.1584%/year. The result for the *LengthSt* covariate indicated that for each PV unit that increases the length of a street, the variation of the PR increases, on average, by 0.00117% per elapsed month. As before, this result adds up; thus, for instance, a street with 10 PV units has, on average, a  $\Delta PR\%$  of 0.1264%/year higher than a street that has just one unit. These results were related to the exposure to the local conditions, particularly to the prevailing winds, and suggested ways to improve the PR of PV production units, both for those that are already in operation and for those that could be installed in this (or a similar) place in the future.

Finally, the obtained results were translated to economic terms, in order to quantify their impact so that they could be useful for those stakeholders interested in investing in this type of sustainable energy.

A future line of research will address the effects of the curtailment orders on the energy produced, issued by REE. In this line, we will extend the present study beyond 2019 in terms of energy not produced by renewable sources, as well as their economic and environmental costs, taking into account not only the results presented in this article but the changes in the energy legislation in the Canary Islands.

**Author Contributions:** Conceptualization, C.M., R.D.-G., B.G.-D., S.G.-P., L.O. and E.L.; methodology, C.M., R.D.-G., B.G.-D., S.G.-P., L.O. and E.L.; software, R.D.-G.; validation, C.M., R.D.-G., B.G.-D., S.G.-P., L.O. and E.L.; formal analysis, C.M. and R.D.-G.; investigation, C.M., R.D.-G., B.G.-D., S.G.-P., L.O. and E.L.; resources, C.M., L.O. and E.L.; data curation, C.M. and R.D.-G.; writing—original draft preparation, C.M. and R.D.-G.; writing—review and editing, C.M., R.D.-G., B.G.-D., S.G.-P., L.O. and E.L.; visualization, C.M., R.D.-G., B.G.-D., S.G.-P., L.O. and E.L.; supervision, B.G.-D. and S.G.-P.; project administration, E.L.; funding acquisition, C.M., L.O. and E.L. All authors have read and agreed to the published version of the manuscript.

**Funding:** This research and the APC has been funded by Interreg (V-A-Spain-Portugal (Madeira-Açores-Canarias-MAC) 2014–2020), grant number: MAC2/1.1a/395.

**Institutional Review Board Statement:** Not applicable.

**Informed Consent Statement:** Not applicable.

**Data Availability Statement:** Not applicable.

**Acknowledgments:** This work has been developed within the MACLAB-PV project framework, which has been co-financed by the INTERREG Madeira-Azores-Canarias Territorial Cooperation Programme (MAC) 2014–2020. Second Call. Axis 1—Enhancing research, technological development, and innovation.

**Conflicts of Interest:** The authors declare no conflict of interest.

## References

- Dag, H.I.; Buker, M.S. Performance Evaluation and Degradation Assessment of Crystalline Silicon Based Photovoltaic Rooftop Technologies under Outdoor Conditions. *Renew. Energy* **2020**, *156*, 1292–1300. [[CrossRef](#)]
- Gxasheka, A.R.; van Dyk, E.E.; Meyer, E.L. Evaluation of Performance Parameters of PV Modules Deployed Outdoors. *Renew. Energy* **2005**, *30*, 611–620. [[CrossRef](#)]
- Osterwald, C.R.; Adelstein, J.; del Cueto, J.A.; Sekulic, W.; Trudell, D.; McNutt, P.; Hansen, R.; Rummel, S.; Anderberg, A.; Moriarty, T. Resistive Loading of Photovoltaic Modules and Arrays for Long-Term Exposure Testing. *Prog. Photovolt. Res. Appl.* **2006**, *14*, 567–575. [[CrossRef](#)]
- Polverini, D.; Field, M.; Dunlop, E.; Zaaman, W. Polycrystalline Silicon PV Modules Performance and Degradation over 20 Years. *Prog. Photovolt. Res. Appl.* **2013**, *21*, 1004–1015. [[CrossRef](#)]
- Chamberlin, C.E.; Rocheleau, M.A.; Marshall, M.W.; Reis, A.M.; Coleman, N.T.; Lehman, P.A. Comparison of PV Module Performance before and after 11 and 20 Years of Field Exposure. In Proceedings of the 2011 37th IEEE Photovoltaic Specialists Conference, Seattle, WA, USA, 19–24 June 2011; pp. 101–105.
- da Fonseca, J.E.F.; de Oliveira, F.S.; Prieb, C.W.M.; Krenzinger, A. Degradation Analysis of a Photovoltaic Generator after Operating for 15 Years in Southern Brazil. *Sol. Energy* **2020**, *196*, 196–206. [[CrossRef](#)]
- Pozza, A.; Sample, T. Crystalline Silicon PV Module Degradation after 20 Years of Field Exposure Studied by Electrical Tests, Electroluminescence, and LBIC. *Prog. Photovolt. Res. Appl.* **2016**, *24*, 368–378. [[CrossRef](#)]
- Dhimish, M. Thermal Impact on the Performance Ratio of Photovoltaic Systems: A Case Study of 8000 Photovoltaic Installations. *Case Stud. Therm. Eng.* **2020**, *21*, 100693. [[CrossRef](#)]
- Gopi, A.; Sudhakar, K.; Keng, N.W.; Krishnan, A.R. Comparison of Normal and Weather Corrected Performance Ratio of Photovoltaic Solar Plants in Hot and Cold Climates. *Energy Sustain. Dev.* **2021**, *65*, 53–62. [[CrossRef](#)]
- Dhimish, M. Performance Ratio and Degradation Rate Analysis of 10-Year Field Exposed Residential Photovoltaic Installations in the UK and Ireland. *Clean Technol.* **2020**, *2*, 170–183. [[CrossRef](#)]
- Kaaya, I.; Lindig, S.; Weiss, K.-A.; Virtuani, A.; Sidrach de Cardona Ortin, M.; Moser, D. Photovoltaic Lifetime Forecast Model Based on Degradation Patterns. *Prog. Photovolt. Res. Appl.* **2020**, *28*, 979–992. [[CrossRef](#)]
- Liu, Z.; Castillo, M.L.; Youssef, A.; Serdy, J.G.; Watts, A.; Schmid, C.; Kurtz, S.; Peters, I.M.; Buonassisi, T. Quantitative Analysis of Degradation Mechanisms in 30-Year-Old PV Modules. *Sol. Energy Mater. Sol. Cells* **2019**, *200*, 110019. [[CrossRef](#)]
- Jordan, D.C.; Kurtz, S.R. Photovoltaic Degradation Rates—An Analytical Review. *Prog. Photovolt. Res. Appl.* **2013**, *21*, 12–29. [[CrossRef](#)]
- Richter, M.; Tjengdrawira, C.; Vedde, J.; Green, M.; Frearson, L.; Herteleer, B.; Jahn, U.; Herz, M.; Köntges, M. *Technical Assumptions Used in PV Financial Models Review of Current Practices and Recommendations Technical Assumptions Used in PV Financial Models Review of Current Practices and Recommendations*; International Energy Agency: Paris, France, 2017.
- Ishii, T.; Masuda, A. Annual Degradation Rates of Recent Crystalline Silicon Photovoltaic Modules. *Prog. Photovolt. Res. Appl.* **2017**, *25*, 953–967. [[CrossRef](#)]
- Pascual, J.; Martínez-Moreno, F.; García, M.; Marcos, J.; Marroyo, L.; Lorenzo, E. Long-Term Degradation Rate of Crystalline Silicon PV Modules at Commercial PV Plants: An 82-MWp Assessment over 10 Years. *Prog. Photovolt. Res. Appl.* **2021**, *29*, 1294–1302. [[CrossRef](#)]

17. Rosillo, F.G.; Alonso-García, M.C. Evaluation of Color Changes in PV Modules Using Reflectance Measurements. *Sol. Energy* **2019**, *177*, 531–537. [CrossRef]
18. Piliougine, M.; Oukaja, A.; Sidrach-de-Cardona, M.; Spagnuolo, G. Temperature Coefficients of Degraded Crystalline Silicon Photovoltaic Modules at Outdoor Conditions. *Prog. Photovolt. Res. Appl.* **2021**, *29*, 558–570. [CrossRef]
19. Choi, S.; Ishii, T.; Sato, R.; Chiba, Y.; Masuda, A. Performance Degradation Due to Outdoor Exposure and Seasonal Variation in Amorphous Silicon Photovoltaic Modules. *Thin Solid Films* **2018**, *661*, 116–121. [CrossRef]
20. Makrides, G.; Zinsser, B.; Schubert, M.; Georghiou, G.E. Performance Loss Rate of Twelve Photovoltaic Technologies under Field Conditions Using Statistical Techniques. *Sol. Energy* **2014**, *103*, 28–42. [CrossRef]
21. Alshare, A.; Tashoutsh, B.; Altarazi, S.; El-khalil, H. Energy and Economic Analysis of a 5 MW Photovoltaic System in Northern Jordan. *Case Stud. Therm. Eng.* **2020**, *21*, 100722. [CrossRef]
22. Fuster-Palop, E.; Vargas-Salgado, C.; Ferri-Revert, J.C.; Payá, J. Performance Analysis and Modelling of a 50 MW Grid-Connected Photovoltaic Plant in Spain after 12 Years of Operation. *Renew. Sustain. Energy Rev.* **2022**, *170*, 112968. [CrossRef]
23. Kumar, N.; Pal, N. Location and Orientation Based Performance Analysis of 4.98 KWp Solar Photovoltaic System for Isolated Indian Islands. *Sustain. Energy Technol. Assess.* **2022**, *52*, 102138. [CrossRef]
24. Chikh, M.; Berkane, S.; Mahrane, A.; Sellami, R.; Yassaa, N. Performance Assessment of a 400 KWp Multi-Technology Photovoltaic Grid-Connected Pilot Plant in Arid Region of Algeria. *Renew. Energy* **2021**, *172*, 488–501. [CrossRef]
25. Yang, D. Simulation Study of Parameter Estimation and Measurement Planning on Photovoltaics Degradation. *Int. J. Energy Stat.* **2015**, *03*, 1550013. [CrossRef]
26. Chuang, S.-L.; Ishibashi, A.; Kijima, S.; Nakayama, N.; Ukita, M.; Taniguchi, S. Kinetic Model for Degradation of Light-Emitting Diodes. *IEEE J. Quantum Electron.* **1997**, *33*, 970–979. [CrossRef]
27. Vázquez, M.; Rey-Stolle, I. Photovoltaic Module Reliability Model Based on Field Degradation Studies. *Prog. Photovolt. Res. Appl.* **2008**, *16*, 419–433. [CrossRef]
28. Laird, N.M.; Ware, J.H. Random-Effects Models for Longitudinal Data. *Biometrics* **1982**, *38*, 963–974. [CrossRef]
29. Dethier, V.G. *Climates in Miniature. A Study of Micro-Climate and Environment.* T. Bedford Franklin. *Q. Rev. Biol.* **1956**, *31*, 215–216. [CrossRef]
30. Peel, M.C.; Finlayson, B.L.; McMahon, T.A. Updated World Map of the Köppen-Geiger Climate Classification. *Hydrol. Earth Syst. Sci.* **2007**, *11*, 1633–1644. [CrossRef]
31. ITER, S.A. Inversor Teide 100. Available online: <https://www.iter.es/wp-content/uploads/2016/01/Ficha-técnica-Inversor-Teide-100.pdf> (accessed on 12 October 2022).
32. Ministerio de Economía Real Decreto 436/2004, de 12 de Marzo. Available online: <https://www.boe.es/buscar/doc.php?id=BOE-A-2004-5562> (accessed on 12 October 2022).
33. Linares, A.; Llarena, E.; Montes, C.; Gonzalez-Diaz, B.; Friend, M.; Cendagorta, M. Three Years Operating 24 MW PV Grid-Connected Facilities in Tenerife (Canary Islands, Spain). In Proceedings of the 24th European Photovoltaic Solar Energy Conference and Exhibition, Hamburg, Germany, 1 September 2009.
34. Red Eléctrica. Available online: <https://www.ree.es/es> (accessed on 12 October 2022).
35. Ministerio de Industria, Turismo y Comercio. Real Decreto 661/2007, de 25 de Mayo, Por El Que Se Regula La Actividad de Producción de Energía Eléctrica En Régimen Especial. Available online: <https://www.boe.es/buscar/act.php?id=BOE-A-2007-10556> (accessed on 12 October 2022).